HHS Public Access

Author manuscript

Neurobiol Aging. Author manuscript; available in PMC 2016 July 01.

Published in final edited form as:

Neurobiol Aging. 2015 July ; 36(7): 2241–2247. doi:10.1016/j.neurobiolaging.2015.03.011.

Endogenous murine Aβ increases amyloid deposition in APP23 but not in APPPS1 transgenic mice

Jasmin Mahler[1,2,3], **Jose Morales-Corraliza**[4,5], **Julia Stolz**[1,2,3], **Angelos Skodras**[1,2], **Rebecca Radde**[1], **Carmen C. Duma**[1], **Yvonne S. Eisele**[1,2], **Matthew J. Mazzella**[4], **Harrison Wong**[4], **William E. Klunk**[5,6], **K. Peter R. Nilsson**[7], **Matthias Staufenbiel**[1,2], **Paul M. Mathews**[4,5], **Mathias Jucker**[1,2], and **Bettina M. Wegenast-Braun**[1,2]

[1]Department of Cellular Neurology, Hertie Institute for Clinical Brain Research, University of Tübingen, D-72076 Tübingen, Germany

[2]DZNE, German Center for Neurodegenerative Diseases, D-72076 Tübingen, Germany

[3]Graduate School for Cellular and Molecular Neuroscience, University of Tübingen, D-72074 Tübingen, Germany

[4]Nathan S. Kline Institute for Psychiatric Research, 140 Old Orangeburg Road, Orangeburg, NY 10962, USA

[5]Department of Psychiatry, New York University School of Medicine, New York, NY 10016, USA

[6]Department of Neurology, University of Pittsburgh School of Medicine, Pittsburgh, Pennsylvania 15261, USA

[7]Department of Chemistry, IFM, Linköping University, Linköping, Sweden

Abstract

Endogenous murine amyloid-β peptide (Aβ) is expressed in most Aβ precursor protein (APP) transgenic mouse models of Alzheimer's disease but its contribution to β-amyloidosis remains unclear. We demonstrate ~35% increased cerebral Aβ load in APP23 transgenic mice compared to age-matched APP23 mice on an *App*-null background. No such difference was found for the much faster Aβ-depositing APPPS1 transgenic mouse model between animals with or without the murine *App* gene. Nevertheless, both APP23 and APPPS1 mice co-deposited murine Aβ and immunoelectron microscopy revealed a tight association of murine Aβ with human Aβ fibrils. Deposition of murine Aβ was considerably less efficient compared to the deposition of human Aβ indicating a lower amyloidogenic potential of murine Aβ *in vivo*. The amyloid dyes Pittsburgh

[1]pFTAA = pentamer formyl thiophene acetic acid

Correspondence to **Bettina Wegenast-Braun**bettina.braun@uni-tuebingen.de Phone +49-7071-29-87607 Hertie Institute for Clinical Brain Research Department of Cellular Neurology Otfried-Müller Strasse 27 D-72076 Tübingen Germany or **Mathias Jucker**mathias.jucker@uni-tuebingen.de Phone +49-7071-29-86863 Hertie Institute for Clinical Brain Research Department of Cellular Neurology Otfried-Müller Strasse 27 D-72076 Tübingen Germany.

Compound B and pentamer formyl thiophene acetic acid (pFTAA [1]) did not differentiate between amyloid deposits consisting of human Aβ and deposits of mixed human-murine Aβ. Our data demonstrate a differential effect of murine Aβ on human Aβ deposition in different APP transgenic mice. The mechanistically complex interaction of human and mouse Aβ may affect pathogenesis of the models and should be considered when models are used for translational preclinical studies.

Keywords

Alzheimer's disease; APP transgenic mouse models; Murine APP Knockout; Murine amyloid-beta (Aβ); Beta-Amyloid; Mixed amyloid-beta (Aβ) fibrils

1. INTRODUCTION

Alzheimer's disease (AD) research has strongly benefited from the use of transgenic (tg) mouse models which overexpress human APP carrying disease-linked mutations, often in combination with overexpression of mutated human presenilin 1 or 2 (PS1/2; for review see Duyckaerts et al., 2008). These models develop many of the typical characteristics of cerebral β-amyloidosis due to the overproduction of human Aβ, but generally continue to express endogenous murine Aβ. Only recently, robust cerebral β-amyloidosis was achieved with APP knock-in models harboring several familial AD mutations (Saito et al., 2014).

Murine Aβ differs from its human homologue in three amino acids at residues 5, 10, and 13 (Arg-5 to Gly, Tyr-10 to Phe, and His-13 to Arg; Yamada et al., 1987). *In vitro*, murine Aβ forms mixed amyloid fibers with human Aβ, and such mixed fibers revealed a higher insolubility than pure human Aβ fibers (Fung et al., 2004). In tg mouse models, co-integration of murine and human Aβ in amyloid deposits also occurs (Pype et al., 2003, van Groen et al., 2006, Morales-Corraliza et al., 2013). However, somewhat inconsistent to the *in vitro* findings an increased solubility of the amyloid has been reported when murine Aβ was overexpressed in human APP tg mice (Jankowsky et al., 2007). Consistent with this latter study amyloid deposits isolated from APP tg mice are more soluble than from human AD brain (Kuo et al., 2001, Kalback et al., 2002).

Even though the available data suggest an effect of murine Aβ on amyloidosis, its nature is poorly understood. Given the routine use of APP tg mice as translational models (Jucker, 2010), e.g. to study the effect of amyloid lowering treatments, a better knowledge of the role of murine Aβ in amyloid formation is needed. To this end, we herein compare two APP tg mouse models (APP23 and APPPS1 mice; Sturchler-Pierrat et al., 1997, Radde et al., 2006) on a wildtype versus a murine *App*-null background.

2. METHODS

2.1 Mice

Hemizygous APP23 mice, overexpressing human APP with the Swedish double mutation (K670N/M671L; Sturchler-Pierrat et al., 1997) and hemizygous APPPS1 mice, co-expressing human APP with the Swedish double mutation and human PS1 with the L166P

mutation (Radde et al., 2006) were bred with *App*-null mice (Calhoun et al., 1999). Such breeding generated again (hemizygous) APP23 and (hemizygous) APPPS1 as well as (hemizygous) littermates lacking endogenous murine APP (koAPP23; koAPPPS1). Wildtype littermates were also included in some of the analyses. The human APP transgene was always inherited from the fathers. All mice were bred on a C57BL/6J background and both lines expressed the transgenes under the neuron-specific murine Thy-1 promoter. Only female APP23 and koAPP23 mice were used in this study. As no obvious gender effect was noted for APPPS1 mice, both female and male APPPS1 and koAPPPS1 mice were used. Mice were group housed in specific pathogen-free conditions. All procedures with animals were performed in compliance with protocols approved by the local animal use committee and university regulations.

2.2 Brain processing, immunoblot analysis and ELISA measurements

Mice were deeply anesthetized with isoflurane, decapitated and brains were prepared. Brain hemispheres were dissected for immunohistochemistry (see below) and for biochemical analyses. For the latter, the cerebellum was removed and the tissue was snap-frozen on dry ice and stored at −80°C until use. For Aβ ELISA and immunoblot analyses, the tissue was homogenized at 10% (w/v) in 50 mM Tris (pH 8.0), 150 mM NaCl, 250 mM sucrose and 5 mM EDTA containing proteinase inhibitors (1mM phenylmethylsulfonyl fluoride and LAP Stock Solution (5 μg/ml each leupeptin hemisulfate salt/antipain HCl/pepstatin A in N-N-dimethylformamide)) (Schmidt et al., 2012b). The homogenated brain tissue was aliquoted and stored at −80°C until use.

For Western blot analyses, proteins were separated using 4-20% Tris-HCl SDS-PAGE and transferred onto polyvinylidene difluoride membranes. Membranes were incubated overnight in primary antibody, washed and incubated with horseradish peroxidase-conjugated IgG for 1 hour (h). ECL substrate was added and proteins were visualized by exposure to x-ray films (Morales-Corraliza et al., 2009). Both human and murine APP and CTF levels were detected by our in-house monoclonal antibody C1/6.1 and murine APP and sAPPα were recognized by the in-house monoclonal antibody m3.2 (Morales-Corraliza et al., 2009). Monoclonal anti-β-tubulin antibody (Sigma-Aldrich, St. Louis, MI) was used as an internal loading control. Diethylamine extraction was used for mice analyzed before Aβ deposition had started (‘pre-depositing’ mice including 1.5-month-old APP23, koAPP23, APPPS1 and koAPPPS1 mice) while formic acid extraction was used for Aβ depositing mice (including 14.5 month-old APP23 and koAPP23 and 3 month-old APPPS1 and koAPPPS1 mice). Aβ levels were determined by sandwich ELISA (Schmidt et al., 2012a). Aβ was captured with carboxy-terminal monoclonal antibodies, which recognize exclusively either Aβ40 (JRF/cAβ 40/10) or Aβ42 (JRF/c Aβ42/26), see Rozmahel *et al*. (2002) for original description of these antibodies. In combination with these antibodies, horseradish peroxidase-conjugated JRF/Aβ/N25 was used to detect human Aβ and horseradish peroxidase-conjugated JRF/rAβ 1-15/2 for murine Aβ (Schmidt et al., 2012a). ELISA results are reported as the mean ± standard error of the mean (SEM) in fmol of Aβ per g wet brain, based on standard curves using synthetic Aβ1-40 and Aβ1-42 peptide standards (American Peptide Co. Sunnyvale, CA).

2.3 Histology and immunohistochemistry

Brain hemispheres for immunohistochemistry were immersion fixed in 4% paraformaldehyde (PFA) in phosphate-buffered saline (PBS) for 2 days, cryoprotected in 30% sucrose in PBS for 2 days and frozen in methylbutane on dry ice. Hemibrains were serially cut into 40 μm thick coronal sections with a freezing-sliding microtome. Immunohistochemical staining was performed according to standard immunoperoxidase procedures using an Elite ABC kit (Vector Laboratories, Burlingame, California, USA) and Vector SG (Vector Laboratories) as a substrate. In general, Aβ deposits were stained using the polyclonal antibody CN3 (1:1000) raised against synthetic human Aβ1–16 peptide (Eisele et al., 2010). Sections were counterstained with Congo Red according to standard protocols.

2.4 Fluorescent double labeling for murine Aβ and pFTAA

Immunofluorescent staining of murine Aβ was performed on 40 μm coronal sections according to a customized immunolabeling protocol. Unspecific binding sites were blocked in three steps: first with anti-mouse blocking serum (Vector Laboratories M.O.M. blocking reagent, 1h, room temperature (RT)), second with skim milk powder (3% (w/v) solution in dH_2O, 15 min, RT), and third with standard blocking solution (0,15% (v/v) Triton x-100 and 5% (v/v) horse serum in Tris-buffered saline (TBS), 1h, RT). The murine Aβ-specific monoclonal m3.2 antibody (see 2.2) was used as a primary antibody (stock solution 1.33 mg/ml, diluted 1:500 in TBS) and incubated at 4°C over night. An anti-mouse biotinylated secondary antibody (Vector Laboratories, Vectastain mouse IgG; 1:250) was incubated for 2h at RT and detected with a streptavidin based fluorescent detection system (ATTO647N, ATTO-Tec GmbH, Siegen, Germany; 1:500, 1h, RT). Staining with pFTAA (1.5 mM in deionized water, 1:1000 in TBS) was performed similar to a previous description (Klingstedt et al., 2011).

2.5 Image acquisition

Mosaic overview images of CN3/Congo Red-stained sections were acquired on a Zeiss Axioplan 2 microscope with an Axiocam HRm (Carl Zeiss MicroImaging GmbH, Jena, Germany) using a 4x objective (0.1 NA, Carl Zeiss MicroImaging GmbH) in combination with the MosaiX function of the Axiovision 4.7 software (Carl Zeiss MicroImaging GmbH). High-magnification images were acquired with a 20x objective (0.5 NA, Carl Zeiss MicroImaging GmbH). Images depicting pFTAA-/ immuno-double labeling were taken with the Zeiss LSM 510 META (Axiovert 200M) confocal microscope. Laser lines 458 and 633 were used to excite pFTAA and ATTO647N, respectively. To depict the whole structure of interest, some images were acquired as z-stacks, and maximum-intensity projections are shown as indicated.

2.6 Spectral analysis of pFTAA-stained Aβ plaques

Amyloid staining with pFTAA was performed as described above. Spectra were acquired on a Zeiss LSM 510 META (Axiovert 200M) confocal microscope (40x oil-immersion objective, 1.3 NA) equipped with a spectral detector. The dye was excited using the 458 nm argon laser line; emission spectra were acquired from 470 nm to 695 nm and normalized to

their respective maxima. Spectra were obtained from 3 regions of interest (ROIs) within each plaque core.

2.7 Stereological analysis

The total Aβ load was quantified on a CN3/Congo Red-stained set of every 12th systematically sampled coronal section. Cortical brain regions were defined using a standard mouse brain atlas. Stereological analysis was performed using a microscope (Axioskop, Carl Zeiss MicroImaging GmbH) equipped with a motorized xyz-stage coupled to a video-microscopy system (Microfire, Optronics, California, USA). The investigators who performed the analysis were blind to the sample genotypes. The total Aβ load (expressed as percent of total cerebral cortex) was determined by calculating the areal fraction occupied by the Congo Red staining in addition to the CN3 staining, however only if not already counted as CN3-positive, in two-dimensional sectors (20x objective, 0.45 NA; Calhoun et al., 1998).

2.8 Immuno Electron Microscopy

For electron microscopy mice were perfused transcardially with 0.1 M PBS followed by 0.1% glutaraldehyde and 4% PFA in PBS. Brains were removed and postfixed overnight in 4% PFA in PBS. 150 μm coronal slices were cut and dehydrated in a graded series of increasing ethanol concentrations (30%, 50%, 70%, 95% and 100% of ethanol respectively; Schwarz and Humbel, 2007). Sections were embedded in Lowicryl K11M and placed between 2 ACLAR films cut into a slide shape (200 μm thick). Pieces of brain tissue (neocortex) were removed with a scalpel and re-embedded in Durcupan blocks (Fluka, Steinheim, Germany). Using an ultramicrotome (Ultracut, Leica, Bensheim, Germany) serial ultrathin sections (50 nm) were cut. Grids with serial ultrathin sections were rinsed in blocking buffer (0.2% gelatin, 0.5% bovine serum albumin in 0.1 M PBS) at RT (Stalder et al., 2001). Polyclonal anti-Aβ antibody NT12 (a previous version of CN3) and monoclonal m3.2 were detected with 18 nm gold-coupled secondary goat-anti-rabbit antibody (Jackson ImmunoResearch Europe Ltd., Newmarket, Suffolk, UK) or 10 nm gold-coupled secondary goat-anti-mouse antibody (Yorkshire Bioscience Ltd, Heslington, York, UK), respectively. Sections were contrasted with 1% aqueous uranyl acetate for 3 min.

2.9 Quantitative postmortem binding of [3H]PIB

Binding to brain homogenates was performed with slight modifications of a procedure described in detail previously (Klunk et al., 2003). Briefly, frozen tissue was homogenized with a Polytron tissue homogenizer (PT 10/35; Brinkman Instruments, Westbury, NY) at RT for 30 seconds at setting 6 in PBS (137 mM NaCl, 3 mM KCl, 10 mM sodium phosphate, pH 7.0) at a concentration of 10 mg of brain per milliliter. This homogenate was then diluted 10-fold in PBS to 1 mg/ml. [H-3]PIB (1 nM; specific activity, 61.4 Ci/mmol; American Radiolabeled Chemicals, St. Louis, MO) was prepared in 900 μl of PBS and binding was initiated by the addition of 100 μl of the 1 mg/ml brain homogenate (in triplicate), and the samples were incubated at 22°C for 60 min. Nonspecific binding was defined as the number of counts remaining in the presence of 1 μM unlabeled PIB. The binding mixtures were filtered through a Whatman (Maidstone, UK) GF/B glass filter via a Brandel (Gaithersburg, MD) M-24R cell harvester and washed rapidly five times with 3 ml of PBS. The filters were counted in Cytoscint-ES after thorough vortexing. Results were corrected for nonspecific,

nondisplaceable binding in the presence of 1 μM PIB and expressed as the mean ± standard deviation (SD) in picomoles of [3H]PIB bound per g wet tissue weight in the homogenate.

2.10 Statistical analysis

For statistical comparison within groups unpaired Student's t-test was performed. Confidence intervals were set to 95%; significance levels are reported as following: (*) for $p \leq 0.05$, (**) for $p \leq 0.01$, (***) for $p \leq 0.001$. Bonferroni correction was used where required to counteract for multiple comparisons.

3. RESULTS

Hemizygous APP23 and APPPS1 tg mice were bred with *App*-null mice (koAPP) to generate offspring with and without endogenous mouse APP (APP23, koAPP23, APPPS1, koAPPPS1). While APP23 mice overexpress human APP with the Swedish double mutation (K670N/M671L) starting amyloid deposition around 8-10 months of age, APPPS1 mice additionally express human PS1 with the L166P mutation resulting in a very high Aβ42 to Aβ40 ratio and thereby a very early onset of cerebral amyloidosis before the age of 2 months. Protein expression of human and mouse APP was analyzed by Western blot analysis of mice from all the age groups used (Suppl. Fig. 1).

3.1 Endogenous murine Aβ contributes to Aβ load in APP23 mice but not in APPPS1 mice

First, we compared APP23 mice on both backgrounds to test if murine Aβ affects amyloid deposition. In line with a previous report (Calhoun et al., 1999), no obvious differences were visible at first glance with respect to amyloid deposition on anti-Aβ and Congo Red-stained cortical brain sections from APP23 versus koAPP23 mice at 14.5 or 18.5 months of age (Fig. 1A). However, stereological analysis of the total Aβ-positive area revealed a difference between genotypes, with APP23 mice depicting a ~35% increase in β-amyloid load compared to age-matched koAPP23 mice at both 14.5 and 18.5 months of age, which reached significance for the 14.5 month-old group (Fig. 1A). In addition to an increase in the parenchymal β-amyloid load (diffuse and compact Aβ deposits), a ~90-100% increase in vascular βamyloid (cerebral β-amyloid angiopathy, CAA) was observed for APP23 versus koAPP23 mice at both ages. It should be noted that CAA was only a minor component (between 2.5 and 10%) of the respective total Aβ load.

To investigate whether murine Aβ also affects amyloid deposition in a model of more rapid amyloidosis we extended our analysis to APPPS1 mice (Fig. 1B). Although this model has a lower human APP overexpression than APP23 mice (three- versus seven-fold), the onset of amyloidosis is much faster due to the increased Aβ42 concentration. For the same reason CAA is very rare (Radde et al., 2006). Stereological analysis of the total Aβ-positive area showed only small, non-significant differences between the animals with or without the murine *App* gene at 3 (−0.5%) or 6 months (+8.5%) of age (Fig. 1B).

3.2 Robust deposition of murine Aβ in both APP23 and APPPS1 mice

Next, we determined human and murine brain Aβ40 and Aβ42 concentrations at 1.5 as well as at 14.5 (APP23) or 3 (APPPS1) months of age, to assess their contribution to total Aβ deposition (Table 1). Wildtype littermates were included for baseline levels of murine Aβ.

Murine Aβ levels were similar for 1.5 month-old pre-depositing APP23 mice and wildtype littermates. Furthermore, murine Aβ showed no significant effect on the concentrations of human Aβ in APP23 and koAPP23 mice at 1.5 months of age. However, at 14.5 months of age, a 23-25% increase of human Aβ40 and Aβ42 was noted in APP23 versus koAPP23 mice confirming the histological results (although significance was not reached with ELISA). At the same time a strong increase of mouse Aβ was observed indicating its deposition (Table 1). While the Aβ42/40 ratio increased only slightly for human Aβ, a higher increase was found for mouse Aβ indicating a much stronger preferential accumulation of Aβ42 for the murine than the human peptide (1.4 versus 4.5 fold increase). Overall, the deposition of murine Aβ was much less efficient than human Aβ as its percentage decreased dramatically between pre-depositing and depositing animals (28% versus 1.8% of total Aβ, respectively).

For APPPS1 mice the rather high human and mouse Aβ concentrations at 1.5 months indicated that Aβ deposition had already started in this fast depositing model. A significant effect of murine Aβ on human Aβ concentrations was neither found at 1.5 nor at 3 months of age (APPPS1 versus koAPPPS1; Table 1) in agreement with the histological data. A strong increase of murine Aβ with aging suggests its deposition also in this model. Nevertheless, no effect on the amyloid load was observed between APPPS1 and koAPPPS1 mice.

3.3 Murine and human Aβ co-deposit in Aβ plaques in APP23 and APPPS1 mice

The accumulation of murine Aβ in both APP23 and APPPS1 mice prompted us to analyze whether it may be co-deposited with human Aβ in β-amyloid plaques. In both APP tg lines, immunohistological staining with the murine Aβ-specific antibody m3.2 (Fig. 2) closely matched the plaque labeling by the amyloid-specific fluorescent dye pFTAA (Klingstedt et al., 2011). No m3.2 antibody staining was detected in brains of koAPP23 or koAPPPS1 mice.

To provide further evidence for a tight association of murine and human Aβ in amyloid fibrils at ultrastructural level, immunoelectron microscopy was performed with APPPS1 and koAPPPS1 mice. Results revealed amyloid fibrils labeled with antibodies specific for murine and with antibodies specific for human Aβ. The close association of the two labels indicates the formation of mixed fibrils (Fig. 3).

3.4 Human and mixed Aβ fibrils show similar amyloid dye binding

The tight association of human and murine Aβ in amyloid fibrils may result in conformational changes as compared to fibrils composed of purely human Aβ. In an attempt to identify such changes we tested the binding of amyloid-specific dyes, i.e. the positron emission tracer Pittsburgh Compound B (PIB) as well as the conformation-sensitive dye, pFTAA. For this analysis, we used APPPS1 mice, which depicted a high percentage of co-

deposited murine Aβ (Table 1), but with an overall comparable amyloid load. AD brain tissue was included in the PIB analysis as mixed fibrils may underlie the inefficient binding of PIB to plaques from APP tg mice (Klunk et al., 2005). However, no significant difference for PIB binding to amyloid fibrils with and without murine Aβ was found (Table 2). The brain homogenate from an AD patient with heavy cerebral Aβ deposition yielded higher binding confirming the differential binding of PIB to human and mouse derived amyloid (Table 2), which is apparently independent of murine Aβ. In line pFTAA, which has been shown to detect different plaque morphotypes (Lord et al., 2011, Fritschi et al., 2014) did not reveal any differences in the spectral signature of plaques from APPPS1 versus koAPPPS1 mice (imaging was performed on 3 month-old APPPS1 and koAPPPS1 mice; n=5 /group; 12-15 Aβ plaques per animal were analyzed; data not shown).

4. DISCUSSION

Most human APP tg mouse models of AD generate endogenous murine Aβ together with tg human Aβ. Yet the role of the murine peptide in amyloid formation is not well understood. Here, we demonstrate a ~35% increase of cerebral β-amyloid load in 14.5 month-old APP23 compared to koAPP23 mice lacking endogenous mouse APP and Aβ. A similar trend was observed in 18.5 month-old mice. At both ages, parenchymal plaques and CAA were elevated with an even stronger increase of the less frequent CAA. Determination of human Aβ40 and Aβ42 concentrations in brain homogenates confirmed the difference in insoluble Aβ between APP23 and koAPP23 mice at 14.5 months but did not reveal such a difference for non-deposited Aβ in 1.5 month-old mice. This indicates that murine Aβ affects amyloid deposition as opposed to Aβ generation. In contrast to APP23, neither the amyloid load nor the human Aβ concentrations differed significantly between APPPS1 and koAPPPS1 mice. In a previous study, mouse APP has been overexpressed in APPswe/PS1dE9 mice with amyloidosis intermediate between APP23 and APPPS1. This resulted solely in an increase in CAA but no faster or larger plaque deposition (Jankowsky et al., 2007). Taken together, the data show that the impact of mouse Aβ on amyloidosis differs among APP tg mice and seems to decrease in more aggressive models.

Nevertheless, our data also show an increase of murine Aβ40 and Aβ42 in the brains of plaque bearing APPPS1 mice as compared to pre-depositing and non-tg animals. This indicates accumulation of mouse Aβ even in APPPS1 mice, where the overall amyloid deposition remained unchanged. This surprising finding was confirmed by immunohistology showing murine Aβ in amyloid plaques and by immunoelectron microscopy demonstrating a tight association of human and murine Aβ in amyloid fibrils. The results are in agreement with studies suggesting the formation of mixed human-murine fibrils *in vitro* (Fung et al., 2004) and the co-deposition (Pype et al., 2003, van Groen et al., 2006) or co-immunoprecipitation (Morales-Corraliza et al., 2013) of murine and human Aβ from mouse brain.

Murine Aβ appears to co-deposit from the very first onset of amyloid deposition as an increase in its concentration is already detected in 1.5 month-old APPPS1 mice compared to age-matched non-tg controls, in line with observations in APP/PS mice (van Groen et al., 2006). However, murine Aβ deposition is far less pronounced than human Aβ because it

decreases relative to total Aβ from ~28% in pre-depositing APP23 to ~1.8% in 14.5 month-old mice. The difference seems smaller in APPPS1 mice but pre-deposition data are missing, as first amyloid deposits are already present at 1.5 months in this model. Nonetheless, our data from both models suggest a lower disposition of murine Aβ to deposit *in vivo* than of its human homologue. In this context the changes in Aβ42/40 ratios with amyloid deposition are interesting. While human Aβ42 in APP23 increases 1.5-fold over human Aβ40, mouse Aβ42 accumulates about 4.5-fold over murine Aβ40. A pronounced increase in the murine Aβ42/40 ratio also occurs in APPPS1 mice although its magnitude cannot be assessed due to the missing baseline. These observations confirm the higher amyloidogenic potential of Aβ42 versus Aβ40 *in vivo*. Moreover, they suggest that this potential comes to bear much more with murine Aβ because of its generally lower disposition to accumulate. We therefore hypothesize that the relative increase in total Aβ42 levels in the APP23 mice due to the presence of additional mouse Aβ42 helps to drive/initiate plaque deposition in comparison to koAPP23 mice. Conversely, this effect might be negligible in a mouse model with a per se high Aβ42 concentration like the APPPS1 mice.

We have analyzed the binding characteristics of two amyloid dyes, PIB and the conformation-sensitive dye pFTAA, to human and mixed human-mouse amyloid fibrils in order to test if potential structural differences might be detectable. Even though amyloid from APPPS1 mouse brain with the highest murine Aβ percentage was used no binding differences were found although minor differences below the detection limit of the herein tested dyes cannot be excluded. Interestingly, however, PIB showed similar binding to pure human and mixed human-mouse amyloid fibrils from koAPPPS1 or APPPS1 mice whereas binding to human AD amyloid fibrils was much higher. These results demonstrate that co-deposition of murine Aβ is not the reason for insufficient PIB binding in APP tg mouse models as discussed before (Klunk et al., 2005).

While the aggregation of human mutant tau was accelerated in the absence of murine tau (Ando et al., 2010), implying an anti-aggregation effect of endogenous murine tau, we could herein show that this is not the case for endogenous murine Aβ, which rather contributes to amyloid deposition in human APP tg mouse models. Nevertheless, overexpression of murine APP/Aβ was so far unable to initiate plaque deposition in mice (e.g. Jankowsky et al., 2007). Our present results suggest that this is related to the lower amyloidogenic potential of murine as compared to human Aβ which is indicated by the relatively low deposition of murine Aβ (1.8% of total Aβ at 14.5 months) as compared to its much higher abundance in pre-depositing APP23 mice (28% of total Aβ at 1.5 month).

In summary, our data indicate a differential effect of murine Aβ on amyloid deposition in different APP tg mouse models of AD. Moreover, the amount of mouse Aβ co-deposited does not directly correlate with its effect on amyloid formation. Mouse Aβ, therefore, may affect study outcomes differently in different models and should be addressed in individual lines, before reaching conclusions based on the modeled humanized cerebral amyloidosis.

Supplementary Material

Refer to Web version on PubMed Central for supplementary material.

Acknowledgements

We would like to thank the members of our department including U. Obermüller, C. Krüger, and A. Bosch for assistance and technical support. Special thanks to H. Schwarz (MPI for Developmental Biology, Tübingen) for the ultrastructural analysis. This work was supported by the German Network in Degenerative Dementias (BMBF-01G10705), by the NIA (AG017617 to P.M.M) and a stipend to C.D. from the Hertie Foundation, Frankfurt, Germany, K.P.R.N is financed by an ERC Starting Independent Researcher Grant (Project: MUMID) from the European Research Council.

REFERENCES

Ando K, Leroy K, Heraud C, Kabova A, Yilmaz Z, Authelet M, Suain V, De Decker R, Brion JP. Deletion of murine tau gene increases tau aggregation in a human mutant tau transgenic mouse model. Biochem Soc Trans. 2010; 38:1001–1005. [PubMed: 20658993]

Calhoun ME, Burgermeister P, Phinney AL, Stalder M, Tolnay M, Wiederhold KH, Abramowski D, Sturchler-Pierrat C, Sommer B, Staufenbiel M, Jucker M. Neuronal overexpression of mutant amyloid precursor protein results in prominent deposition of cerebrovascular amyloid. Proc Natl Acad Sci U S A. 1999; 96:14088–14093. [PubMed: 10570203]

Calhoun ME, Wiederhold KH, Abramowski D, Phinney AL, Probst A, Sturchler-Pierrat C, Staufenbiel M, Sommer B, Jucker M. Neuron loss in APP transgenic mice. Nature. 1998; 395:755–756. [PubMed: 9796810]

Duyckaerts C, Potier MC, Delatour B. Alzheimer disease models and human neuropathology: similarities and differences. Acta Neuropathol. 2008; 115:5–38. [PubMed: 18038275]

Eisele YS, Obermuller U, Heilbronner G, Baumann F, Kaeser SA, Wolburg H, Walker LC, Staufenbiel M, Heikenwalder M, Jucker M. Peripherally applied Abeta-containing inoculates induce cerebral beta-amyloidosis. Science. 2010; 330:980–982. [PubMed: 20966215]

Fritschi SK, Cintron A, Ye L, Mahler J, Buhler A, Baumann F, Neumann M, Nilsson KP, Hammarstrom P, Walker LC, Jucker M. Abeta seeds resist inactivation by formaldehyde. Acta neuropathologica. 2014; 128:477–484. [PubMed: 25193240]

Fung J, Frost D, Chakrabartty A, McLaurin J. Interaction of human and mouse Abeta peptides. J Neurochem. 2004; 91:1398–1403. [PubMed: 15584916]

Jankowsky JL, Younkin LH, Gonzales V, Fadale DJ, Slunt HH, Lester HA, Younkin SG, Borchelt DR. Rodent A beta modulates the solubility and distribution of amyloid deposits in transgenic mice. J Biol Chem. 2007; 282:22707–22720. [PubMed: 17556372]

Jucker M. The benefits and limitations of animal models for translational research in neurodegenerative diseases. Nat Med. 2010; 16:1210–1214. [PubMed: 21052075]

Kalback W, Watson MD, Kokjohn TA, Kuo YM, Weiss N, Luehrs DC, Lopez J, Brune D, Sisodia SS, Staufenbiel M, Emmerling M, Roher AE. APP transgenic mice Tg2576 accumulate Abeta peptides that are distinct from the chemically modified and insoluble peptides deposited in Alzheimer's disease senile plaques. Biochemistry. 2002; 41:922–928. [PubMed: 11790115]

Klingstedt T, Aslund A, Simon RA, Johansson LB, Mason JJ, Nystrom S, Hammarstrom P, Nilsson KP. Synthesis of a library of oligothiophenes and their utilization as fluorescent ligands for spectral assignment of protein aggregates. Org Biomol Chem. 2011; 9:8356–8370. [PubMed: 22051883]

Klunk WE, Lopresti BJ, Ikonomovic MD, Lefterov IM, Koldamova RP, Abrahamson EE, Debnath ML, Holt DP, Huang GF, Shao L, DeKosky ST, Price JC, Mathis CA. Binding of the positron emission tomography tracer Pittsburgh compound-B reflects the amount of amyloid-beta in Alzheimer's disease brain but not in transgenic mouse brain. J Neurosci. 2005; 25:10598–10606. [PubMed: 16291932]

Klunk WE, Wang Y, Huang GF, Debnath ML, Holt DP, Shao L, Hamilton RL, Ikonomovic MD, DeKosky ST, Mathis CA. The binding of 2-(4′-methylaminophenyl)benzothiazole to postmortem brain homogenates is dominated by the amyloid component. J Neurosci. 2003; 23:2086–2092. [PubMed: 12657667]

Kuo YM, Kokjohn TA, Beach TG, Sue LI, Brune D, Lopez JC, Kalback WM, Abramowski D, Sturchler-Pierrat C, Staufenbiel M, Roher AE. Comparative analysis of amyloid-beta chemical

structure and amyloid plaque morphology of transgenic mouse and Alzheimer's disease brains. J Biol Chem. 2001; 276:12991–12998. [PubMed: 11152675]

Lord A, Philipson O, Klingstedt T, Westermark G, Hammarstrom P, Nilsson KP, Nilsson LN. Observations in APP bitransgenic mice suggest that diffuse and compact plaques form via independent processes in Alzheimer's disease. The American journal of pathology. 2011; 178:2286–2298. [PubMed: 21514441]

Morales-Corraliza J, Mazzella MJ, Berger JD, Diaz NS, Choi JH, Levy E, Matsuoka Y, Planel E, Mathews PM. In vivo turnover of tau and APP metabolites in the brains of wild-type and Tg2576 mice: greater stability of sAPP in the beta-amyloid depositing mice. PLoS One. 2009; 4:e7134. [PubMed: 19771166]

Morales-Corraliza J, Schmidt SD, Mazzella MJ, Berger JD, Wilson DA, Wesson DW, Jucker M, Levy E, Nixon RA, Mathews PM. Immunization targeting a minor plaque constituent clears beta-amyloid and rescues behavioral deficits in an Alzheimer's disease mouse model. Neurobiology of aging. 2013; 34:137–145. [PubMed: 22608241]

Pype S, Moechars D, Dillen L, Mercken M. Characterization of amyloid beta peptides from brain extracts of transgenic mice overexpressing the London mutant of human amyloid precursor protein. J Neurochem. 2003; 84:602–609. [PubMed: 12558980]

Radde R, Bolmont T, Kaeser SA, Coomaraswamy J, Lindau D, Stoltze L, Calhoun ME, Jaggi F, Wolburg H, Gengler S, Haass C, Ghetti B, Czech C, Holscher C, Mathews PM, Jucker M. Abeta42-driven cerebral amyloidosis in transgenic mice reveals early and robust pathology. EMBO Rep. 2006; 7:940–946. [PubMed: 16906128]

Rozmahel R, Huang J, Chen F, Liang Y, Nguyen V, Ikeda M, Levesque G, Yu G, Nishimura M, Mathews P, Schmidt SD, Mercken M, Bergeron C, Westaway D, St George-Hyslop P. Normal brain development in PS1 hypomorphic mice with markedly reduced gamma-secretase cleavage of betaAPP. Neurobiology of aging. 2002; 23:187–194. [PubMed: 11804702]

Saito T, Matsuba Y, Mihira N, Takano J, Nilsson P, Itohara S, Iwata N, Saido TC. Single App knock-in mouse models of Alzheimer's disease. Nature neuroscience. 2014; 17:661–663.

Schmidt SD, Mazzella MJ, Nixon RA, Mathews PM. Abeta measurement by enzyme-linked immunosorbent assay. Methods Mol Biol. 2012a; 849:507–527. [PubMed: 22528112]

Schmidt SD, Nixon RA, Mathews PM. Tissue processing prior to analysis of Alzheimer's disease associated proteins and metabolites, including Abeta. Methods Mol Biol. 2012b; 849:493–506. [PubMed: 22528111]

Schwarz H, Humbel BM. Correlative light and electron microscopy using immunolabeled resin sections. Methods in molecular biology. 2007; 369:229–256. [PubMed: 17656754]

Stalder M, Deller T, Staufenbiel M, Jucker M. 3D-Reconstruction of microglia and amyloid in APP23 transgenic mice: no evidence of intracellular amyloid. Neurobiology of aging. 2001; 22:427–434. [PubMed: 11378249]

Sturchler-Pierrat C, Abramowski D, Duke M, Wiederhold KH, Mistl C, Rothacher S, Ledermann B, Burki K, Frey P, Paganetti PA, Waridel C, Calhoun ME, Jucker M, Probst A, Staufenbiel M, Sommer B. Two amyloid precursor protein transgenic mouse models with Alzheimer disease-like pathology. Proc Natl Acad Sci U S A. 1997; 94:13287–13292. [PubMed: 9371838]

van Groen T, Kiliaan AJ, Kadish I. Deposition of mouse amyloid beta in human APP/PS1 double and single AD model transgenic mice. Neurobiol Dis. 2006; 23:653–662. [PubMed: 16829076]

Yamada T, Sasaki H, Furuya H, Miyata T, Goto I, Sakaki Y. Complementary DNA for the mouse homolog of the human amyloid beta protein precursor. Biochem Biophys Res Commun. 1987; 149:665–671. [PubMed: 3322280]

HIGHLIGHTS

- Endogenous murine Aβ modulates human Aβ deposition in APP23 transgenic mice.
- No significant effect of murine Aβ on human Aβ deposition in APPPS1 transgenic mice.
- Co-deposition of murine Aβ with human Aβ in amyloid plaques of both mouse models.
- Murine Aβ may affect study outcomes differently in APP transgenic mouse models.

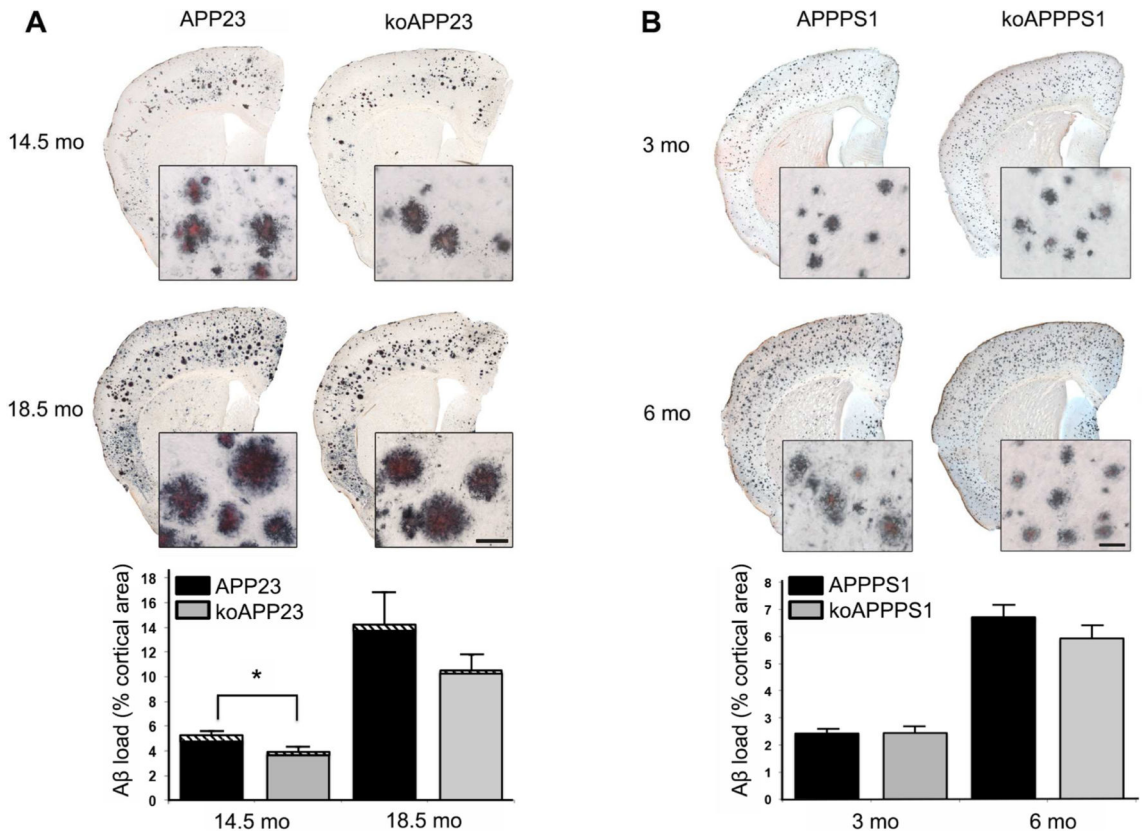

Figure 1. Aβ load in APP23 versus koAPP23 mice and APPPS1 versus koAPPPS1 mice

(A) Representative images of cortical brain sections from 14.5 and 18.5 month-old APP23 and koAPP23 mice stained with an antibody specific for Aβ (CN3) in combination with Congo Red. Inserts represent higher magnification of cortical plaques (Scale bar is 50 μm). Stereological analysis of total Aβ load (CN3/Congo Red-positive area as percentage of total cerebral cortex; 14.5 months: n=9 APP23, n=9 koAPP23, unpaired t-test, p=0.015; 18.5 month: n=4 APP23, n=6 koAPP23, unpaired t-test, p=0.19; error bars: SEM). The striped area at the top of the bars represents the percentage of vascular β-amyloid. **(B)** Representative images of cortical brain sections from 3 and 6 month-old APPPS1 and koAPPPS1 mice stained with an antibody specific for Aβ (CN3) in combination with Congo Red. Inserts represent higher magnification of cortical plaques (Scale bar is 50 μm). Stereological analysis of the Aβ-load (CN3/Congo Red-positive area as percentage of total cerebral cortex; 3 months: n=8 APPPS1, n=7 koAPPPS1, unpaired t-test, p=0.97; 6 months: n=8 APPPS1, n=6 koAPPPS1, unpaired t-test, p=0.44; error bars: SEM). The very minor amount of vascular amyloid at 6 months of age is not visible in the respective graphs.

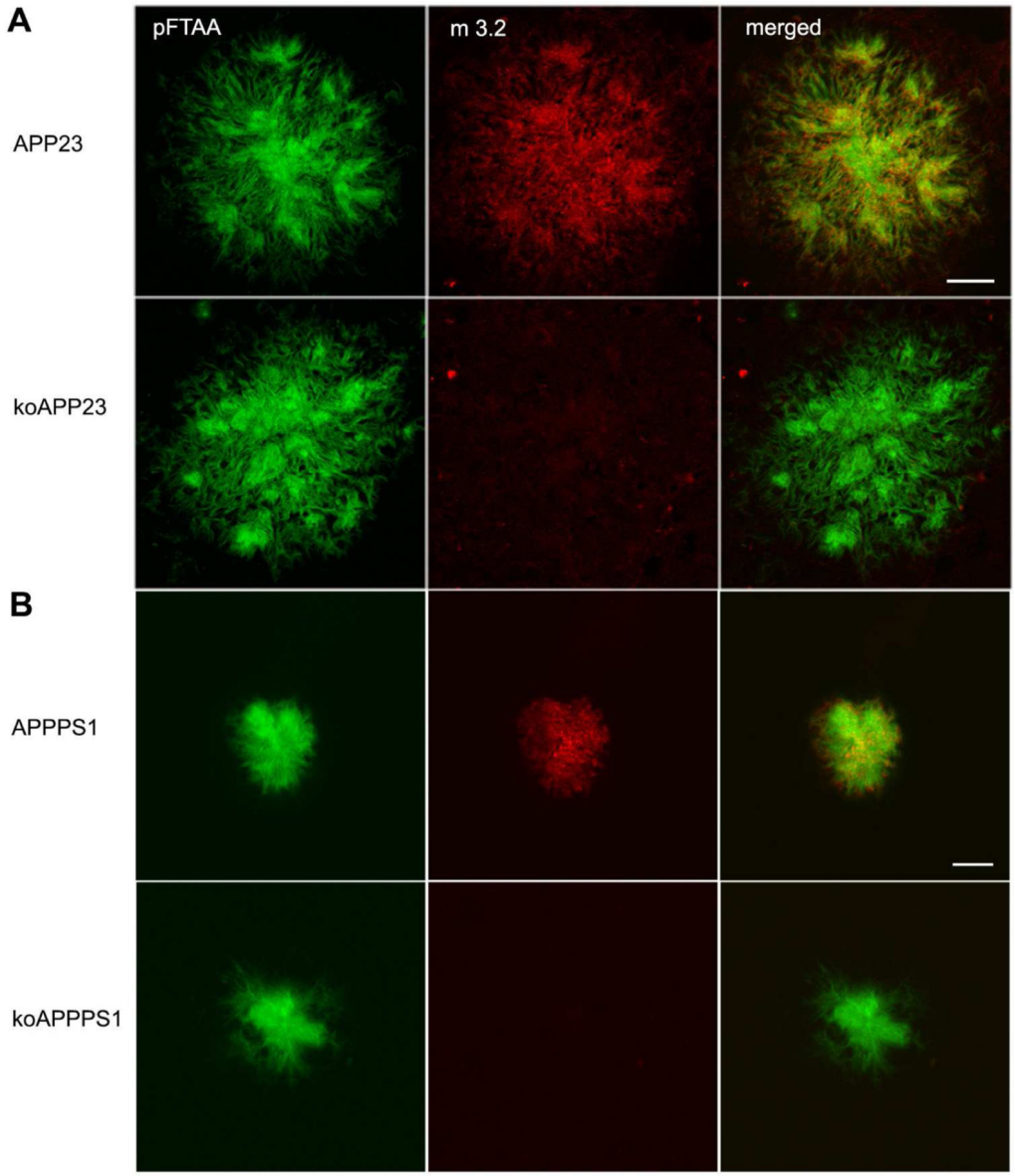

Figure 2. Murine Aβ is part of Aβ plaques of APP23 and APPPS1 mice

Immunohistological staining for murine Aβ (m3.2 antibody) revealed its localization in Aβ plaques of 14.5 month-old APP23 **(A)** and 3 month-old APPPS1 **(B)** mice. Plaques were counter-stained with the amyloid-specific fluorescent dye pFTAA. As expected, no staining of murine Aβ was observed in koAPP23 and koAPPPS1 mice. Two representative animals were examined for each group (4 brain sections/animal). Scale bar is 20 μm for (A) and 10 μm for (B). Images in (B) represent maximum intensity projections of six z-planes each.

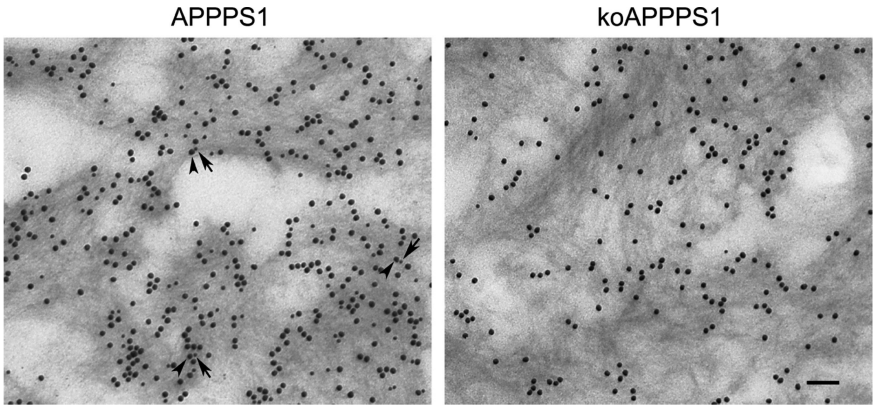

Figure 3. Co-localization of murine and human Aβ in amyloid fibrils

Electron micrograph revealing a tight association of 10 nm gold-decorated murine Aβ (arrows) and 18 nm (arrowheads) gold-decorated human Aβ in amyloid fibrils within the neocortex of a 15 month-old APPPS1 mouse. koAPPPS1 control sections exhibit no murine Aβ immunoreactivity. One representative animal was examined for each group (30-40 pictures were analyzed/animal). Scale bar is 100 nm.

Table 1

Human and murine Aβ levels in various APP transgenic lines

Genotype	Age [mo]	Human Aβ 42 [fmol/g]	Human Aβ 40 [fmol/g]	Human 42:40 Ratio	Murine Aβ 42 [fmol/g]	Murine Aβ 40 [fmol/g]	Murine 42:40 Ratio	% murine Aβ of total Aβ
wt	1.5				70 ± 17	482 ± 49	0.14 ± 0.03	
ko APP23	1.5	272 ± 82	1,265 ± 295	0.21 ± 0.03				
APP23	1.5	176 ± 27	1,090 ± 171	0.16 ± 0.01	65 ± 8	413 ± 48	0.17 ± 0.03	28.40 ± 3.46
ko APP23	14.5	4,524,981 ± 342,125	20,640,263 ± 2,976,319	0.24 ± 0.02				
APP23	14.5	5,548,173 ± 595,479	25,765,046 ± 4,007,354	0.23 ± 0.02	217,098 ± 8,667	302,720 ± 24,780	0.76 ± 0.08	1.82 ± 0.23
ko APPPS1	1.5	4,317 ± 181	2,955 ± 123	1.48 ± 0.11				
APPPS1	1.5	4,549 ± 264	2,934 ± 150	1.55 ± 0.05	1,369 ± 61	357 ± 28	3.98 ± 0.34	18.88 ± 0.73
ko APPPS1	3	2,010,752 ± 190,640	871,106 ± 64,927	2.31 ± 0.15				
APPPS1	3	2,088,929 ± 128,362	710,791 ± 42,286	2.96 ± 0.11	289,347 ± 15,161	25,181 ± 2060	11.80 ± 0.63	10.14 ± 0.34

Human and murine Aβ42 and Aβ40 levels were assessed by ELISA. Non-tg wildtype (wt) mice were included for baseline levels of murine Aβ. 6-8 animals were used per group (n=5 for wt mice).

Table 2

Ex vivo PIB binding in APPPS1, koAPPPS1 and human AD sample

Sample	Total cpm	+ 1 μm PIB	Difference	% Specific Binding
AD brain	8517 ± 191	1329 ± 32	7188	84.4
APPPS1	3893 ± 2.1	1383 ± 77	2510	64.5
koAPPPS1	3610 ± 398	1401 ± 42	2209	61.2

The binding efficiency of the PET tracer PIB was measured in brain samples from an AD patient and 8.5-9.5 month-old APPPS1 and koAPPPS1 mice. Results for AD brain and APPPS1 mice are in line with previous findings (Klunk et al., 2005).